Preliminary Results from 22dec03 Continuum Mapping Scan Pattern Tests with the GBT

Brian Mason 12feb04

1. Implementation

Brian Mason & Richard Prestage wrote a GO procedure in GLISH to prototype Daisy scanning. This was quite straightforward. The only subtelty was figuring out how to represent the desired trajectory in terms of the overconstrained position-velocity-acceleration (PVA) interface the antenna requires. Below I present a simple formalism.

Consider a single dimension x, and a desired continuous trajectory $x(t)$. In our case there is a parametric form for $x(t)$

$$x(t) = r_0 \, cos \, \Omega t \, sin \omega t. \tag{1}$$

which is convenient. The antenna interface requires discretely sampled arrays of x_i, v_i and a_i, all defined at a set of times t_i $(i = 1...N)$. Furthermore the accelerations a_i is contrained to be constant between a_i and a_{i+1}. Note that $a_i = a(t_i)$ does not give the desired trajectory when the accelerations are held constant between steps.

We first require $x_i = x(t_i)$ and fill the x_i array from our parametric form Eq 1. We next specify the initial velocity v_1, again from the explicit derivative of the parametric form evaluated at t_1, $v_1 = v(t_1)$. At this point the trajectory is fully specified, *i.e.* no new information is required. With piecewise constant accelerations the x_i, v_i, and a_i are related as

$$x_{i+1} = x_i + v_i \, (t_{i+1} - t_i) + \frac{1}{2} a_i (t_{i+1} - t_i)^2 \tag{2}$$

With this equation and our initial condition for v_1 we can inductively solve for the a_i and the rest of the v_i. We find

$$v_{i+1} = 2 \frac{x_{i+1} - x_i}{(t_{i+1} - t_i)} - v_i \tag{3}$$

$$a_i = 2 \frac{x_{i+1} - x_i}{(t_{i+1} - t_i)^2} - 2 \frac{v_i}{(t_{i+1} - t_i)} \tag{4}$$

I have implicitly assumed that the antenna interface aims to achieve the x_i and v_i values at the *beginnings* of the primary scan segments. These formulas would be slightly different were that not the case.

In the notation of the memo "Daisy Scan Modes for the GBT": τ is the period of the radial (fastest) modulation; ω is the angular frequency of the radial motion $\omega = 2\pi/\tau$; and Ω is the angular frequency of the basis vector rotation, taken to be $\Omega = \omega/\pi$. The power spectrum of a well-executed daisy scan will then have power at $\Omega \pm \omega$ or, in terms of frequency, $\nu = (1 \pm 1/\pi)/\tau$. For $\tau = 60\,\mathrm{sec}$

these frequencies are 0.0220 and 0.0114 Hz. For $r = 7'$ and $\tau = 60sec$ typical peak velocities are 0.01 deg/sec (slightly greater than characteristic celestial tracking rate of ~ 0.004 deg/sec) and typical peak accelerations are 0.001 deg/sec^2 (much greater than accelerations generated in celestial tracking).

More sophisticated things like Don Well's jerk minimization have been proposed and merit investigation. This is discussed below.

2. Observations

On 12dec03 we did some test observations during PTCS test time. These observations are summarized in full at `http://wiki.gb.nrao.edu/bin/view/PTCS/TPTCSRMP031222`. The weather was poor, and we did only X and Ku-band observations for the daisy-scans. During this run the Quadrant Detector (QD) was collecting data which we use to assess feedarm excitations. We also took test daisy-scan observations, including Q-band data, on 29dec (project TPTCSRMP031229) but we aren't confident the Quadrant Detector was working properly during these observations. Also the winds were well above the accepted Q-band limit of $5m/s$. We don't consider these later data here. A selection of the 22/23 dec data are summarized in Table 1.

Initially we attempted daisy scans with a radial period τ of 30 seconds; this motion excited the fundamental of the structure (peak-to-peak of $\sim 0.02\,\mathrm{V} \sim 2''$) and we decided to abort and scale back to a slower $\tau = 60$ sec.

Also note that only the first *two* scans (128 & 129) are identified as "daisy" scans in the GO FITS file. After this we changed the GO procedure to record a PROCNAME of RALONGMAP in order that `AIPS++` could read the data.

Scan Number	FITS File root	description
128	2003 12 22 21:25:49	X-band, $\tau = 30$sec, $dT = 0.1sec$, duration= $240sec$, $r = 7'$
136	2003 12 22 22:25:41	X-band, $\tau = 60$sec, $dT = 0.2sec$, duration= 1320, $r = 7'$
167	2003 12 22 23:36:17	Ku-band, $\tau = 60$sec $dT = 0.2sec$, duration= 1320, $r = 3'.1$
169	2003 12 23 00:05:26	Ku-band, $\tau = 60$sec, Az/El, $dT = 0.2sec$, duration= 1320, $r = 3'.1$

Table 1: Selected daisy scans of interest from project `TPTCSRMP031222`. The target in all cases (except the Az/El scan) was 3C48. The left column shows the adopted radial oscillation period τ, scan segment length dT, and scan duration (1320 seconds = 22 minutes, roughly what is needed for a "complete" daisy scan with $\tau = 60sec$).

3. Results

3.1. Scan Execution

The GLISH code largely did its jobs and delivered the desired scan pattern on the sky; see Fig 1. The scan was not perfectly executed, as there are some distortions. These distortions are not present in the Az/El daisy (Fig 2) so we suspect that they are not due to servo errors, but rather to imperfections in coordinate transforms internal to the antenna manager. This is all the more so since the Ra/Dec plot depicts *commanded* Ra and Dec, and the Az/El plot depicts *actual* Az and El, which if anything ought to be less ideal. The actual az/el plot for the Ra/Dec daisy (ie when we were tracking the source) is hard to interpret since the source moves non-negligibly in 22 minutes.

3.2. Feedarm Motions

Raw Quadrant Detector data for scan 136 and 169 are shown in Figs 3 and 4. Visual inspection of the QD data led me to the following conclusions:

- The largest effect in either QD channel (X or Y) is a long-term change over the 22-minute track, possibly due to gravitational sagging of the feedarm which is already in the pointing model. The long-term change is much lower in the az/el scan.
- the second largest effect in the QD data is the transient "ringing" at the beginning of a scan, probably due to a jerky scan start, with a typical amplitude of $0.1\,V$;
- the third largest effect is a roughly scan-synchronous ($\tau \sim 45$ sec, corresponding to the $(1 + 1/\pi)/\tau$ mode of the motion). ringing with a typical amplitude of $0.03\,V$ peak to peak;
- a $\sim 0.8\,Hz$ excitation is also evident in the data with a typical peak to peak level of $0.01\,V$.

With Kim's approximate conversions of $38\,mm/Volt$ for the QD data, and a plate scale of 3 arcseconds per mm, we then expect $1''$ to $3''$ peak to peak excursions in the pointing ignoring scan-start effects. These results are summarized in Table 2.

These conclusions are borne out by looking at the power spectra of the QD data. You must excise the first 30 seconds or so of QD data after the scan start to obtain these results, otherwise the jerky scan start contaminates the power spectrum. After this, the 0.8 Hz mode is generally the most strongly excited. See Figures 5 through 7.

The scan-synchronous term could be due to systemic structural distortions caused by the telescope motion. To more clearly examine this I plotted the binned Quadrant Detector signals versus the azimuth and elevation accelerations (Figures 8 through 10). There is a clear correlation

Effect	Frequency (Hz)	Amplitude (V)	Feedarm Deflection (mm)	Pointing
Sag	$\sim 1/1000$	$0.5\,V$	19	$57''$ (?)
Scan Start Ringing	~ 0.6	0.1	4	$13''$
Quasi-static Distortions	0.02	0.03	1	$3''$
Excited Structural Vibrations	0.8	0.01	0.4	$1''$

Table 2: A summary of effects seen in the quadrant detector data. Interpretations are based on a fixed $38\,mm/Volt$ QD calibration and $3''/mm$ plate scale.

between the Quadrant Detector signal and the acceleration. The strongest correlation is between QD channel X and elevation acceleration. Correlations with azimuthal accelerations are weaker. It should be noted that while the correlations strongly stand out in the binned data, the raw data show much larger scatter and some obvious systematics which we have simply averaged over in this analysis.

At first it seemed likely that the imperfect execution of the Ra/Dec daisy scans might be responsible for the $0.8\,Hz$ excitation seen in the data. However the data from the much cleaner Az/El daisy showed similar $0.01\,V$ peak-to-peak excursions. As might be expected the long-term trend in the QD data is weaker when executed at a fixed Az/El.

3.3. Beammapping Analysis

The X-band data were used to make a beammap. The procedure was

1. split the data from the scan into "ON-source" chunks (where the beam was within 3 FWHM radius of the target source) and "OFF-source" chunks (everything else);
2. subtract a mean and gradient from each on-source chunk;
3. average cal-on and cal-off phases within each on-source chunk, and use the difference as a mean measurement of the cal signal to normalize that chunk;
4. convolutionally grid the data onto a regular Ra/Dec grid.

It is generally good procedure for continuum data to subtract the mean level before calibration, and to use enough cal phases to get a reasonable measurement (so the noise level isn't increased significantly). For the convolutional gridding, a Gaussian kernel was used, with a Gaussian width $\sigma_{kernel} = \sigma_{beam}/3.5$ where σ_{beam} is the Gaussian width of the GBT beam $(FWHM/\sqrt{8\,ln(2)})$. The convolutional gridding is greatly accelerated by zeroing out the kernel for data lying at radii greater than $r = 5\,\sigma_{kernel}$ from a given grid cell, *i.e.* only performing the gridding within a circle of radius $5\,\sigma_{kernel}$ of each grid point. A small subset of the timestream data (before the cal normalization) are shown in Fig 11; the X-band beammap is shown in Fig 12. The beammap has roughly the expected X-band FWHM of $1'.4$. The analysis was done in `MATLAB`. This is not a user package but rather is inteded for quick, easy, and flexible analysis & inspection of the data; better beammap results have been produced from this data by Bill Cotton's `OBIT` package. Note that the map shown is in *commanded* Ra/Dec (which is what is recorded in the FITS file); a better procedure for on-the-fly mapping would be to transform observed az and el — which is also recorded— into actual Ra/Dec (or for beammaps, into delta az/delta el to the source).

4. Summary of Conclusions

- The daisy scan procedure worked as intended. We restricted most of our investigations to fairly slow motions, $\tau = 60\,\mathrm{sec}$. If this could be reduced, the daisy scan would allow significantly more rapid beammaps than is currently possible ($\tau = 60\,sec$ requires 22 minutes, about as long as a conventional raster-scanned beammap). We saw structural excitations at $\tau = 30\,sec$ being a factor of ~ 2 higher than at $\tau = 60\,sec$; perhaps a more sophisticated trajectory calculation which minimizes jerk would permit faster modulations.

- For unknown reasons the commanded positions in az/el offset mode were cleaner than the commanded positions in ra/dec offset mode.

- There are preliminary indications that scan segments of 0.1 sec generate cleaner commanded positions than 0.2 sec segments, but this also should be revisited. (this was not discussed above)

- Scan-synchronous signals in the Quadrant Detector data are clearly seen, and are correlated with acceleration as might be expected of quasi-static structural distortions. The strongest correlation is between the X channel of the Quadrant detector and the elevation acceleration; a Y-channel signal is also seen. The correlation with azimuth acceleration is weaker. Further study is needed to characterize these correlations and determine if they are repeatable (this dataset is a reasonable starting point).

- The heirarchy of significant effects— large to small— seen in the QD data are: long term changes when tracking the sky; jerky scan starts; scan-synchronous distortions; and the excitation of structural resonances.

This or other parametric scan patterns would be a good way to investigate acceleration-correlated pointing errors since: it is easy to tune in specified peak accelerations at specified frequencies well below structural frequencies; it is natural to scan for long periods of time and build up datasets uncorrupted by scan start effects, which sensitively probe the correlations; and it is naturally combined with astronomical data. Unfortunately in this particular case the peak accelerations were at the edges of the pattern, and the acceleration at source-crossings was close to zero. This is easily fixed by using an alternate radial modulation, eg,

$$\vec{p}(t) = \frac{r_o}{2}\,(\hat{x}\,cos\,\Omega t\ + \hat{y} sin\,\Omega t)\,(1 - sin\,\omega t) \tag{5}$$

which places the peak acceleration at the center of the circular region, and also slows down source-crossings.

The magnitude of acceleration-correlated pointing errors suggests that for high-frequency mapping applications it is best to use scan patterns which are largely unaccelerated (for example the truncated billiard ball patterns used at the CSO). Unless these errors can be easily calibrated out, elevation accelerations are to be avoided more than azimuthal accelerations. Others have certainly noted the possible significance of quasi-static distortions of the GBT before.

I thank Kim Constantikes, Richard Prestage, & Don Wells for contributions to this work.

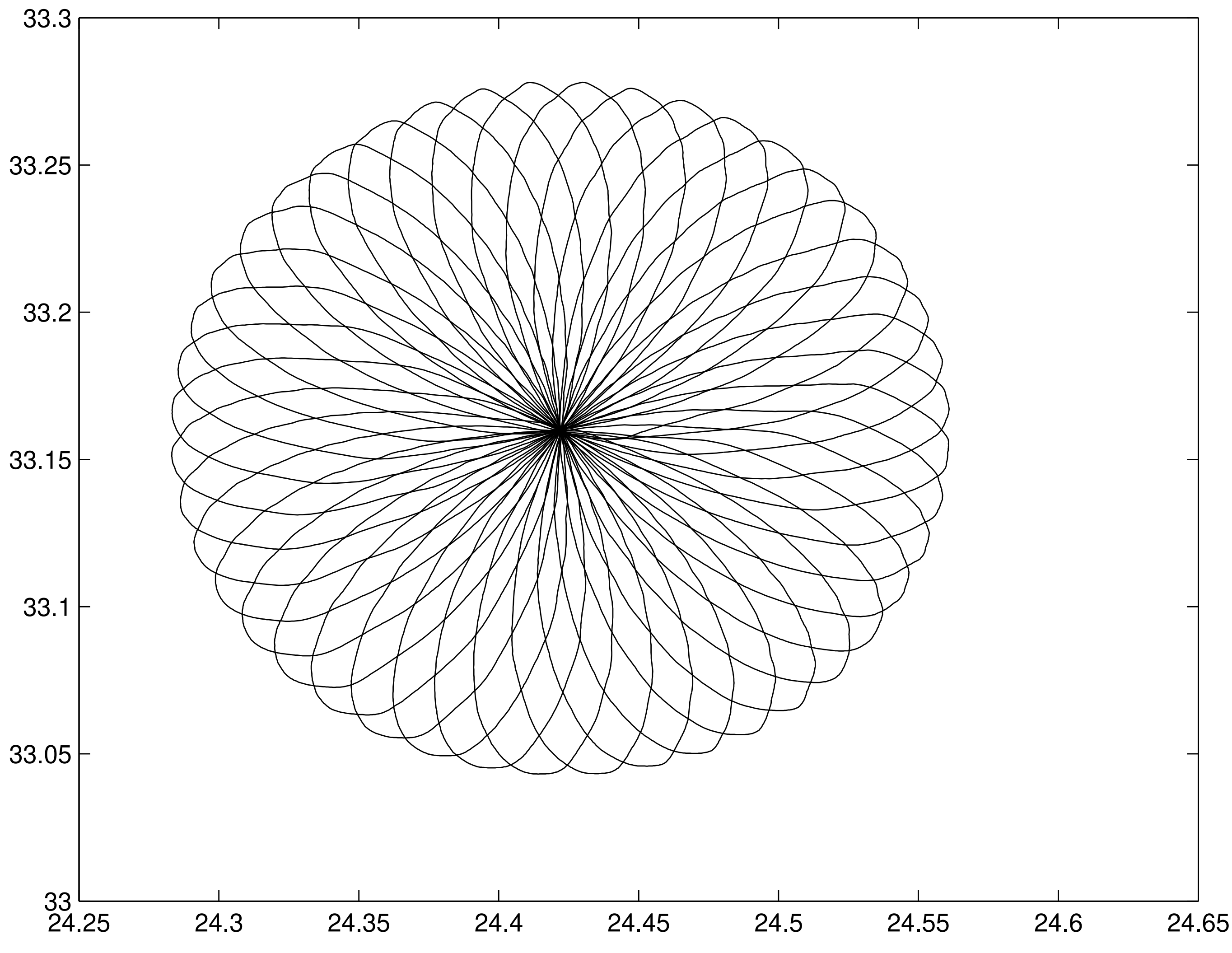

Fig. 1.— Commanded Ra and Dec for a daisy scan (scan number 136) where both the primary and the offset modes were Ra/Dec. The map was centered on the J2000 coordinates of 3C48.

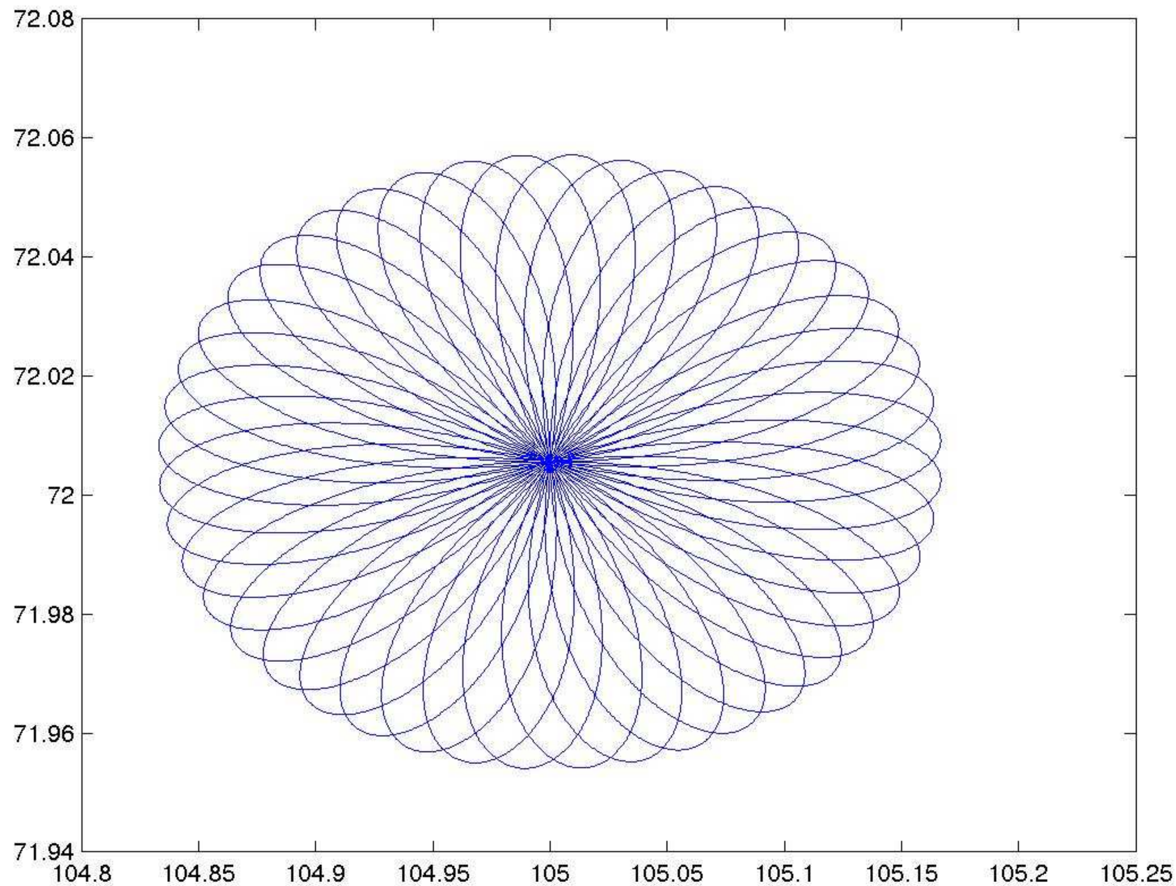

Fig. 2.— Actual achieved az and El for the daisy scan (number 169) where the primary and offset coordinates were both az/el, around a central az/el comparable to those required for 3C48 in this experiment.

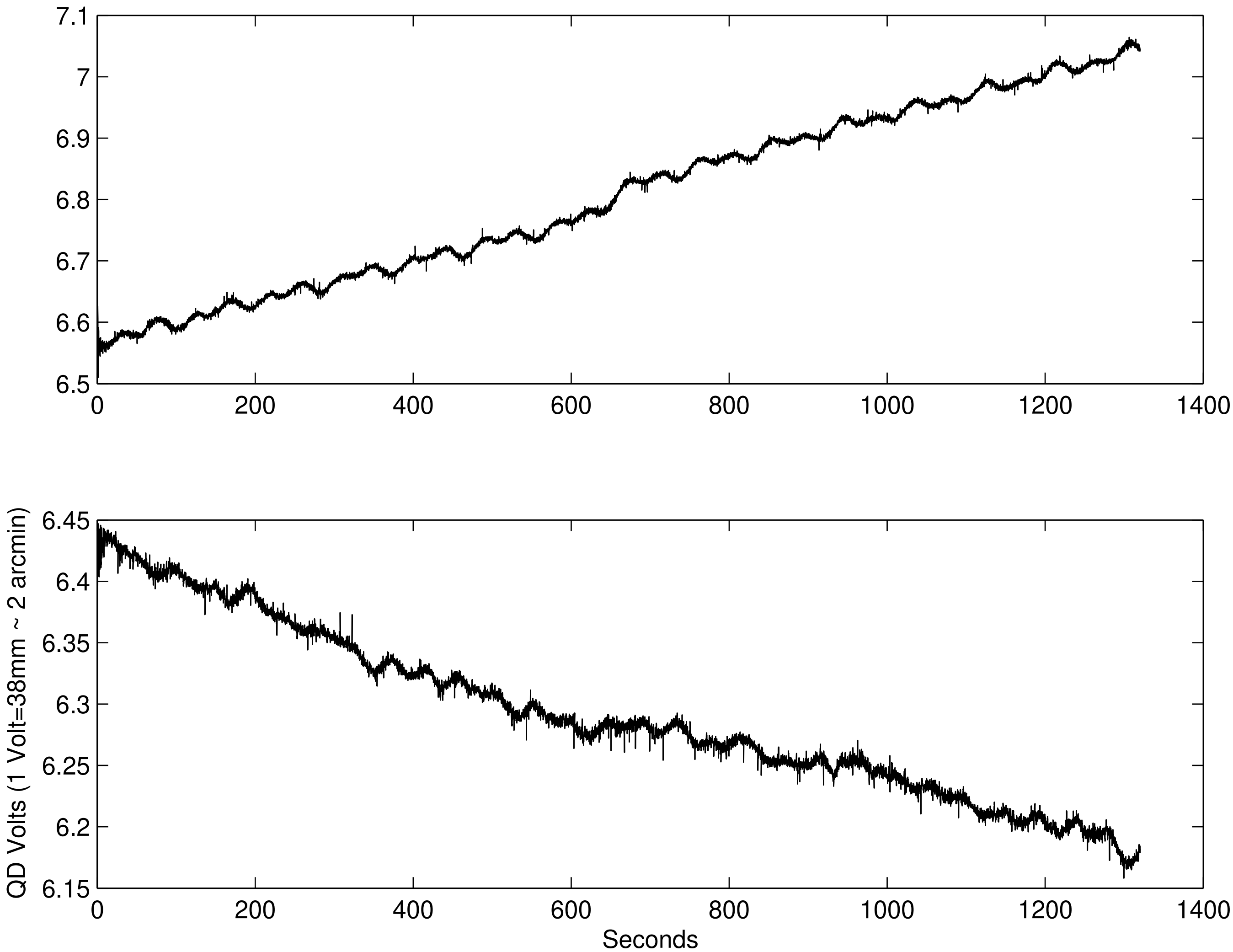

Fig. 3.— Raw Quadrant Detector data for channels X and Y in scan 136 (X-band scan on 3C48). The drift is presumably due to gravitational sag of the feedarm structure relative to the Quadrant Detector mount location. The obvious sinusoidal feature in the data is synchronous with the shortest period of the scan motion $\sim 45\,\mathrm{sec}$.

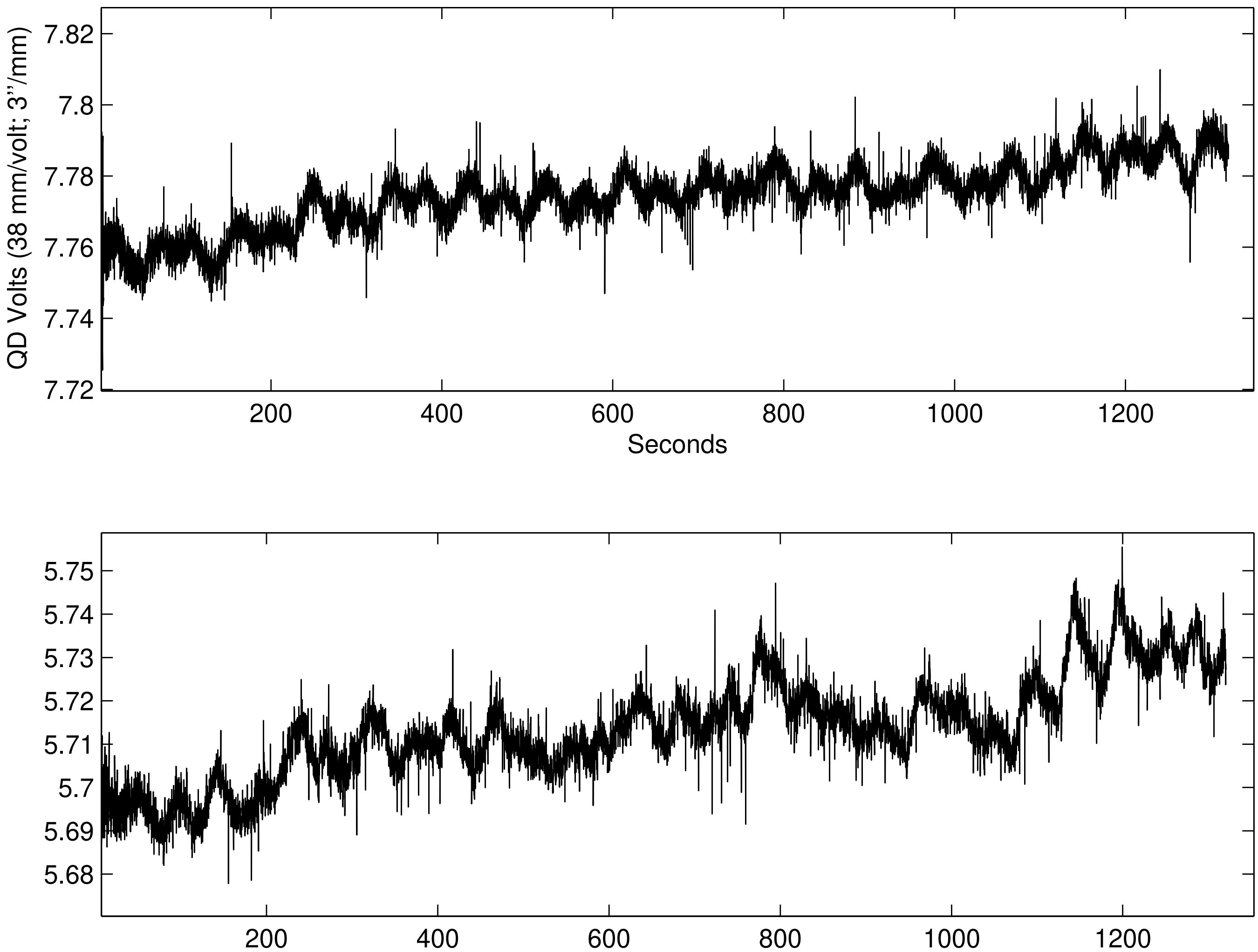

Fig. 4.— Raw Quadrant Detector data for channels X and Y in scan 169 (X-band Az/El scan). Since this scan was at an approximately constant elevation, the much weaker long-term drift is presumed to be due to other effects such as thermal gradients in the telescope structure or QD instability at low frequencies. The obvious sinusoidal feature in the data is synchronous with the shortest period of the scan motion $\sim 45\,\mathrm{sec}$.

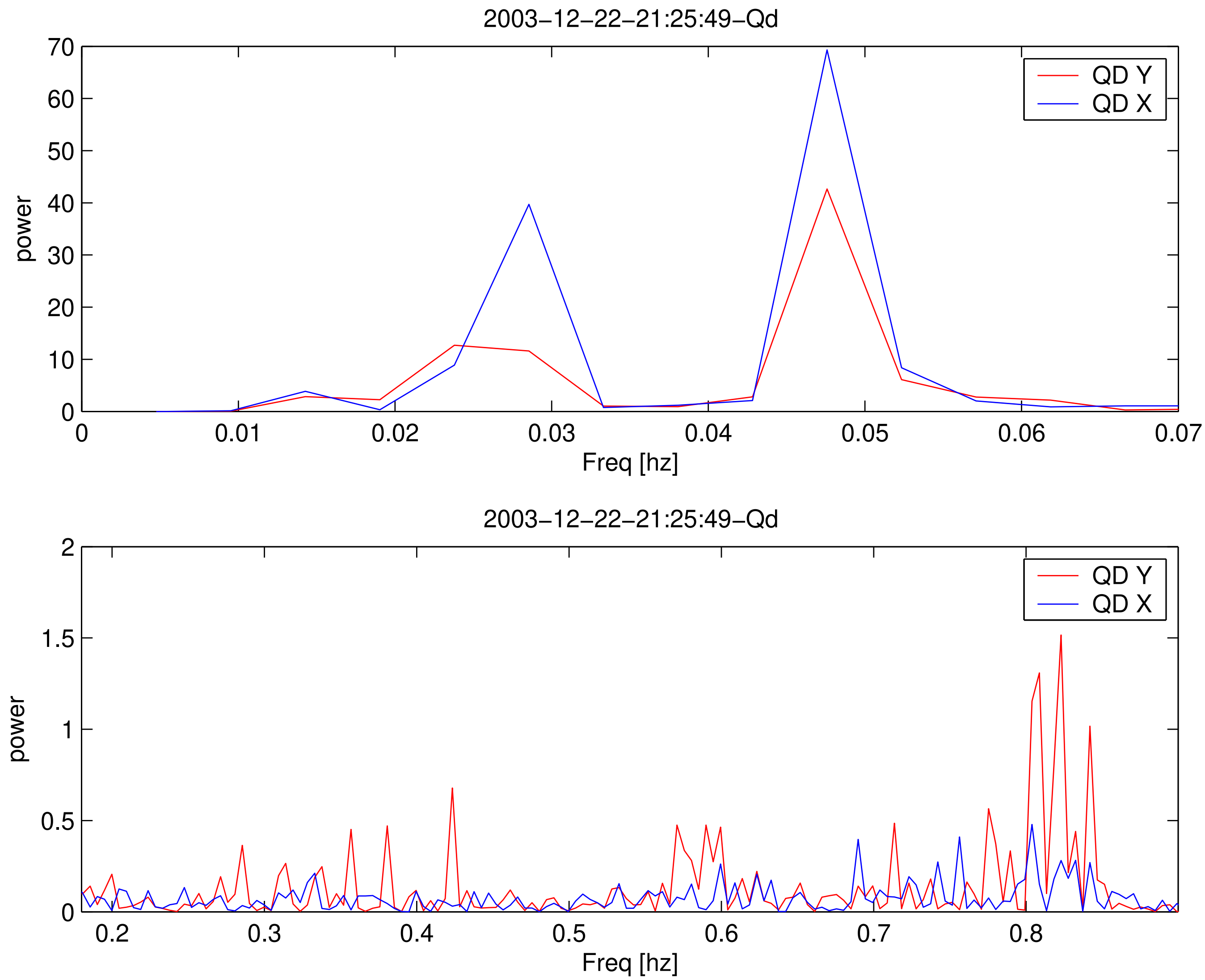

Fig. 5.— Power Spectral Density vs frequency for **Scan 128** ($\tau = 30\,sec$, $r = 7'$, **Ra/Dec**). This scan was shorter than the others so the fourier resolution is lower. The QD data was detrended with a polynomial prior to the FFT.

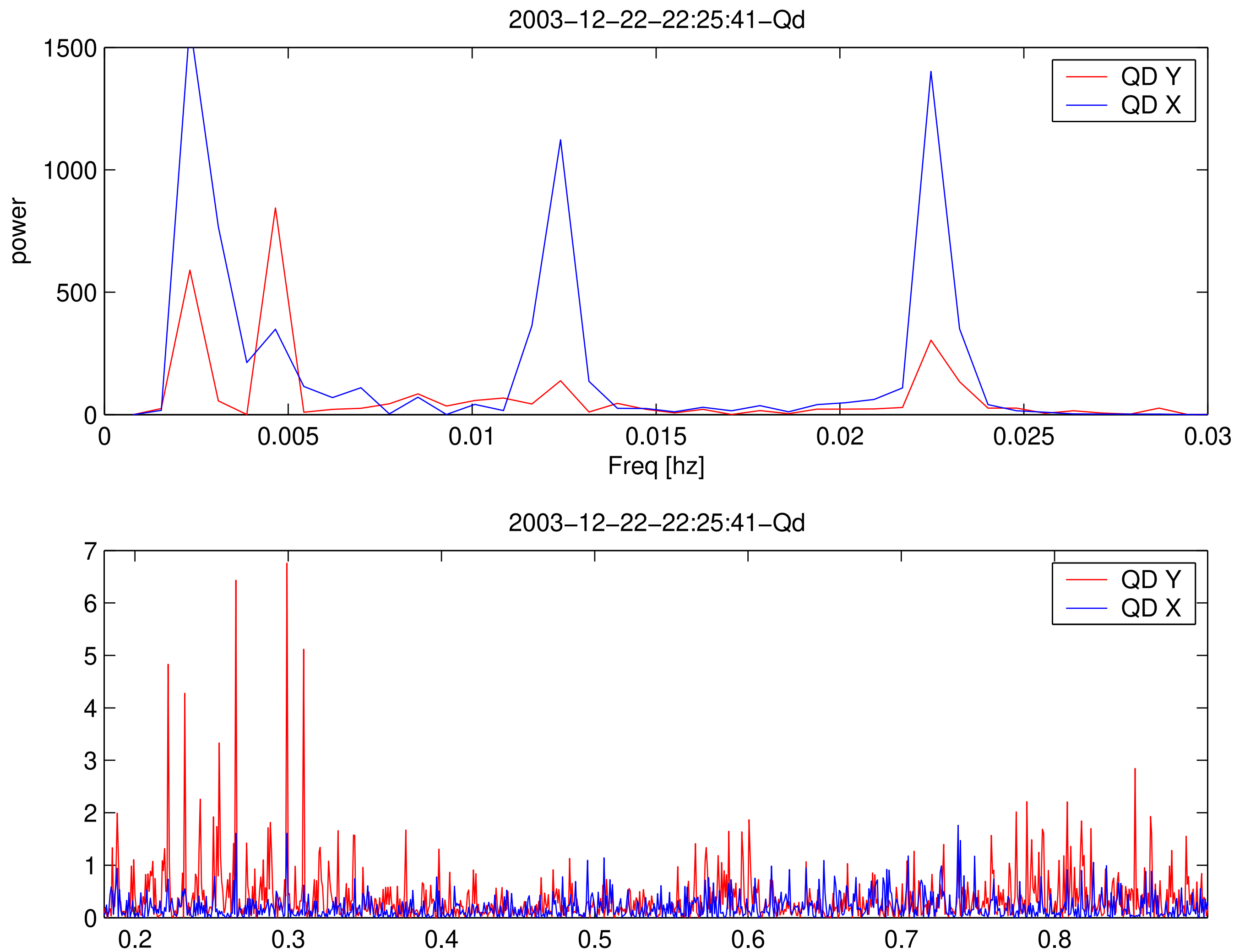

Fig. 6.— Power Spectral Density vs frequency for **Scan 136** ($\tau = 60\,sec$, $r = 7'$, **Ra/Dec**). The QD data was detrended with a polynomial prior to the FFT.

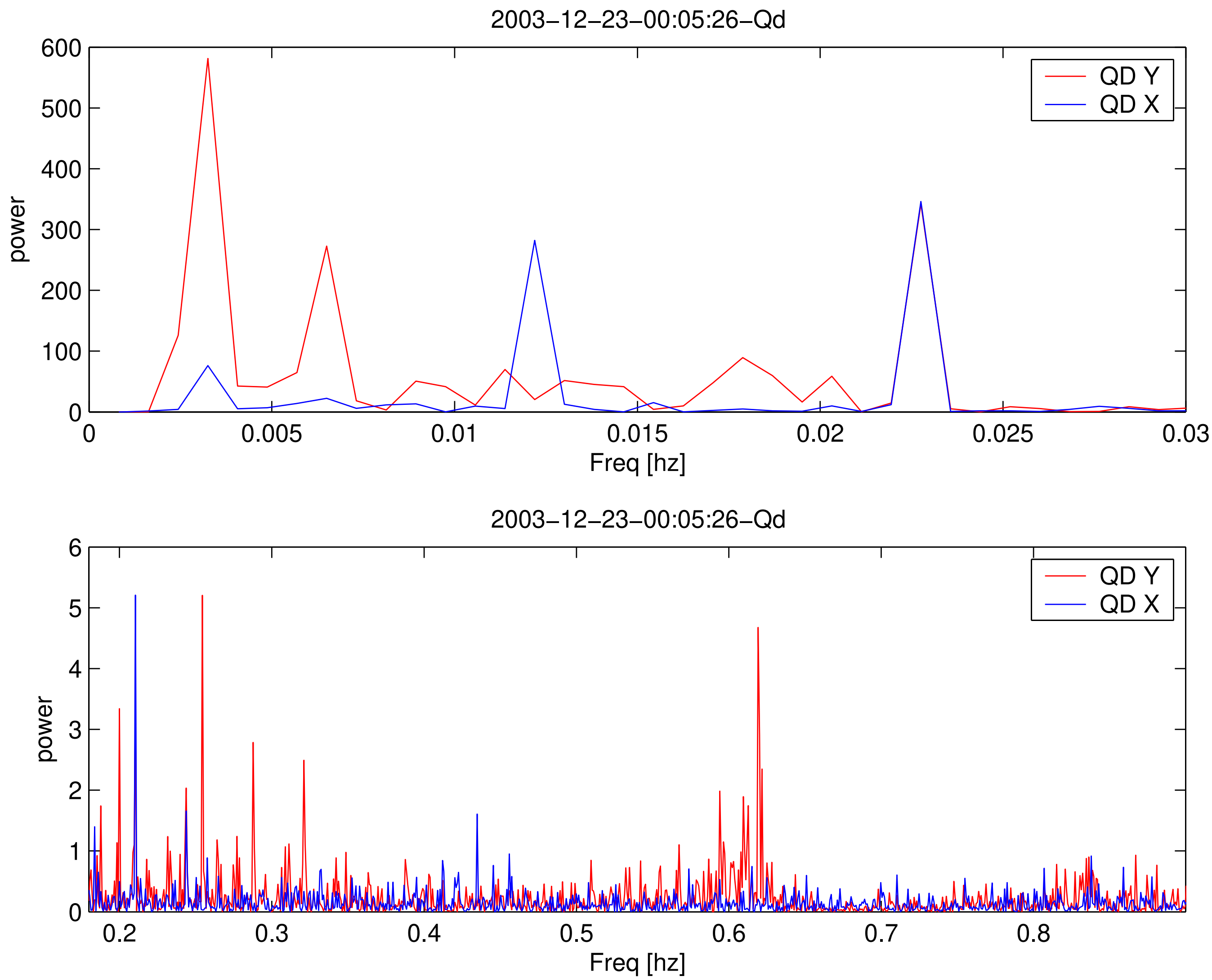

Fig. 7.— Power Spectral Density vs frequency for **Scan 169** ($\tau = 60\,sec$, $r = 3'.1$, **Az/El)**. The QD data was detrended with a polynomial prior to the FFT. In this case the fundamental was the most strongly excited mode, however the scan start here was jerkier than others and that could be the driver.

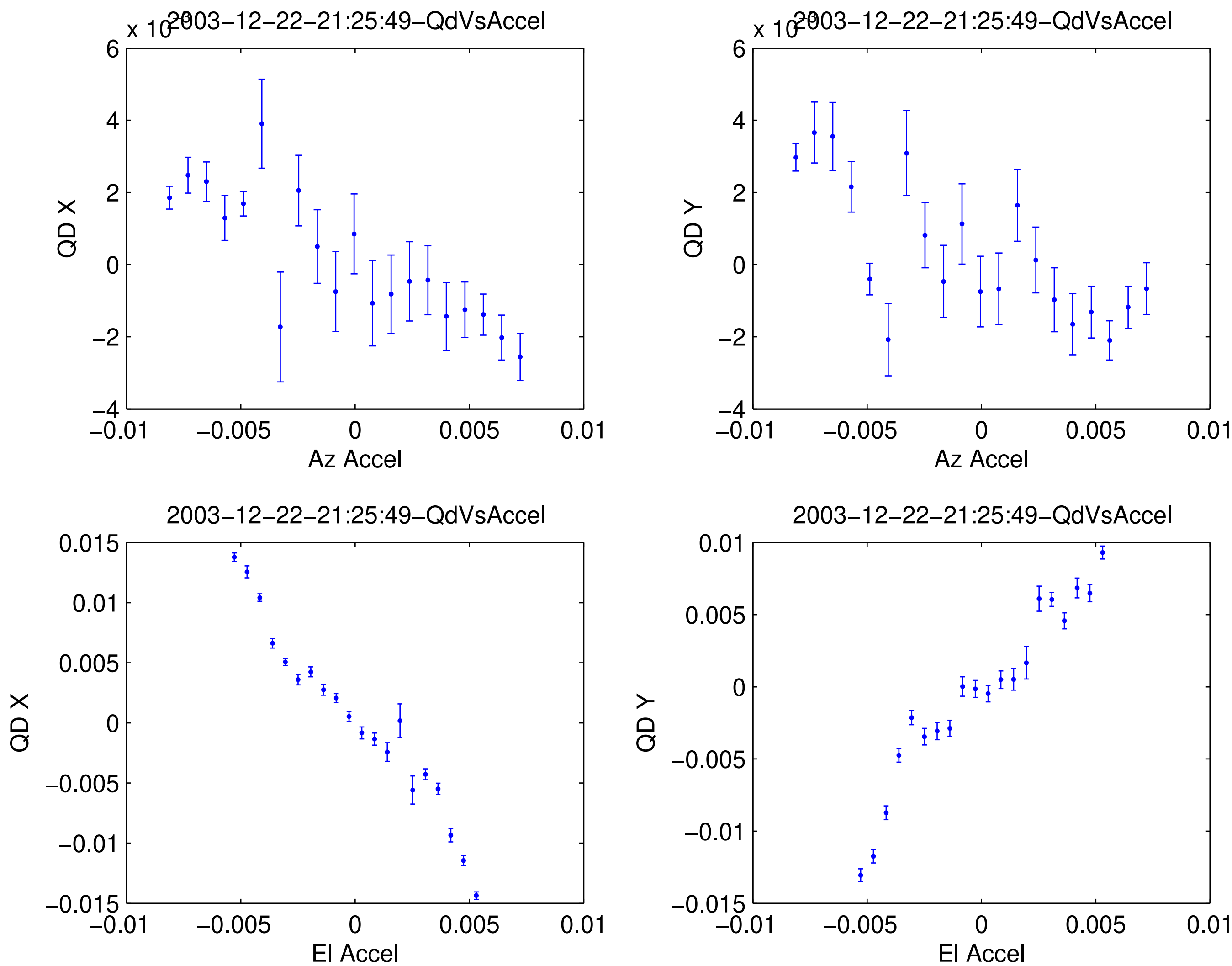

Fig. 8.— QD Data versus acceleration for **Scan 128 (**τ **=** 30 *sec*, r **=** $7'$**, Ra/Dec)**. The accelerations were computed numerically from the observed azimuth and elevation; x-axes are in deg/sec^2, y-axes are in Volts (note: 10^{-3} label is sometimes obscured). QD signals were detrended with a polynomial in time. The central elevation for this scan was $\sim 48°$. This is a short dataset but yields the largest accelerations.

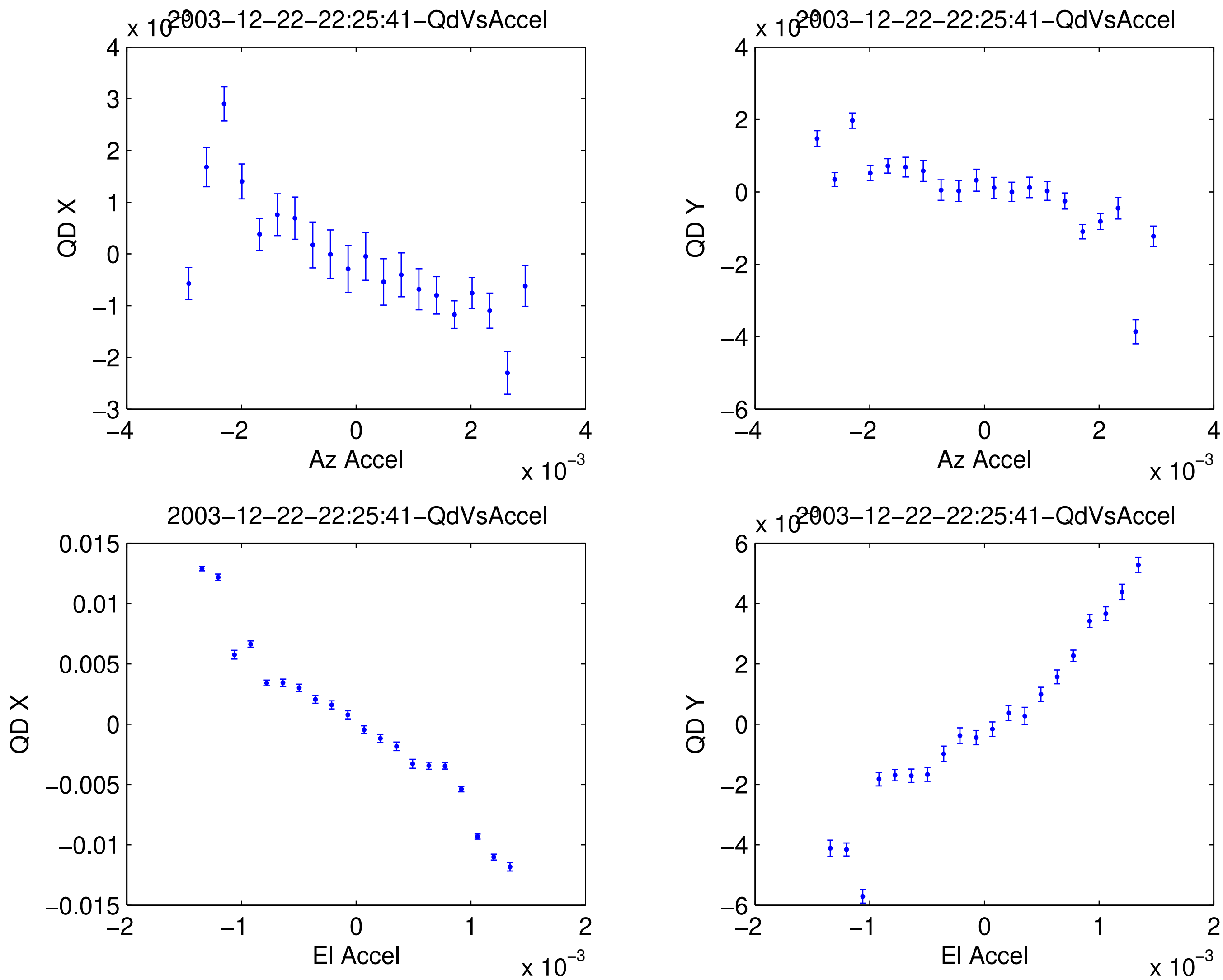

Fig. 9.— **Scan 136 ($\tau = 60\,sec$, $r = 7'$, Ra/Dec)** The accelerations were computed numerically from the observed azimuth and elevation; x-axes are in deg/sec^2, y-axes are in Volts (note: 10^{-3} label is sometimes obscured). QD signals were detrended with a polynomial in time. The central elevation for this scan was $\sim 62°$. This dataset yields moderate accelerations.

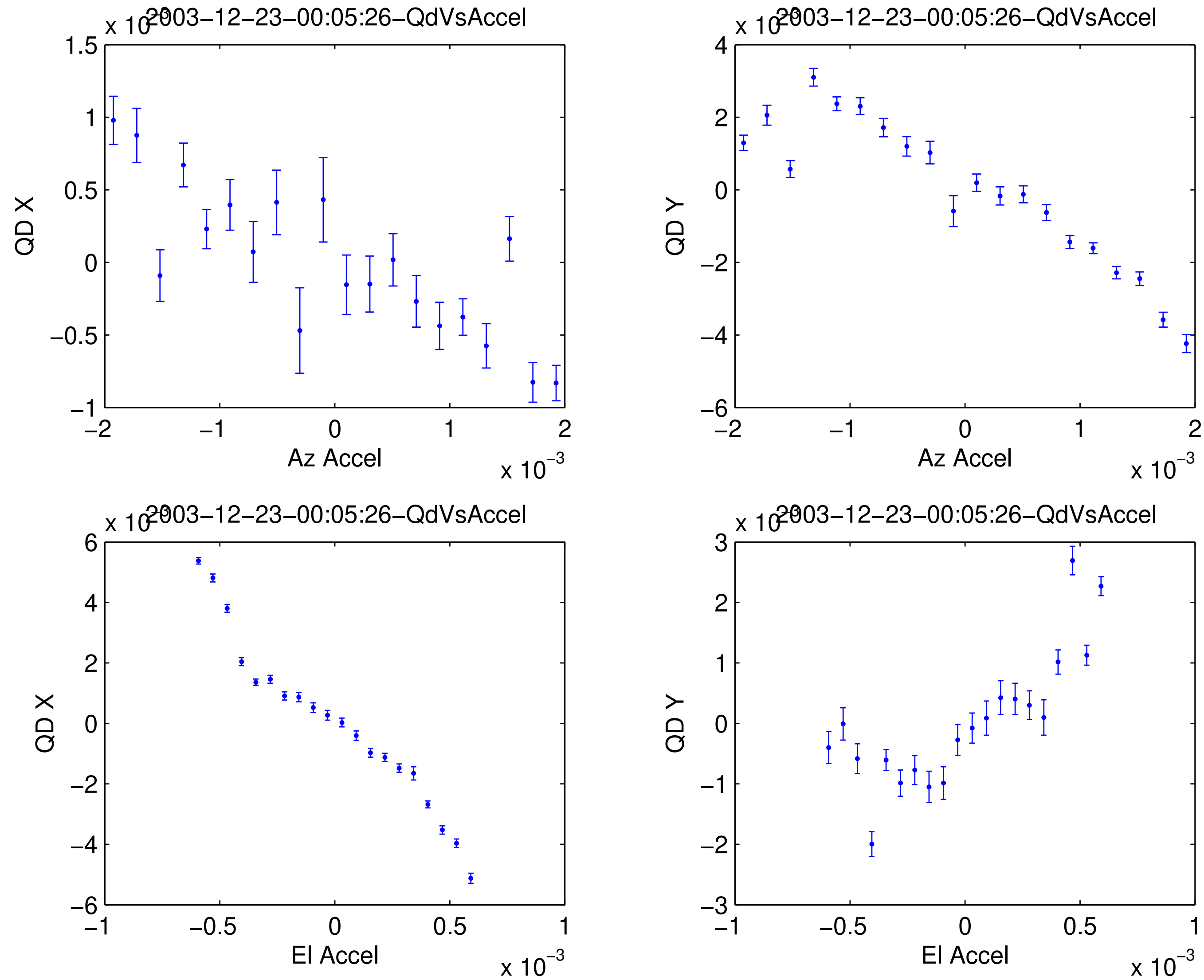

Fig. 10.— **Scan 169 ($\tau = 60\,sec$, $r = 3'.1$, Az/El)** The accelerations were computed numerically from the observed azimuth and elevation; x-axes are in deg/sec^2, y-axes are in Volts (note: 10^{-3} label is sometimes obscured). QD signals were detrended with a polynomial in time. The central elevation for this scan was $\sim 72°$. This dataset yields weaker accelerations than the others, but is potentially less affected by confusing issues since the central az and el were fixed.

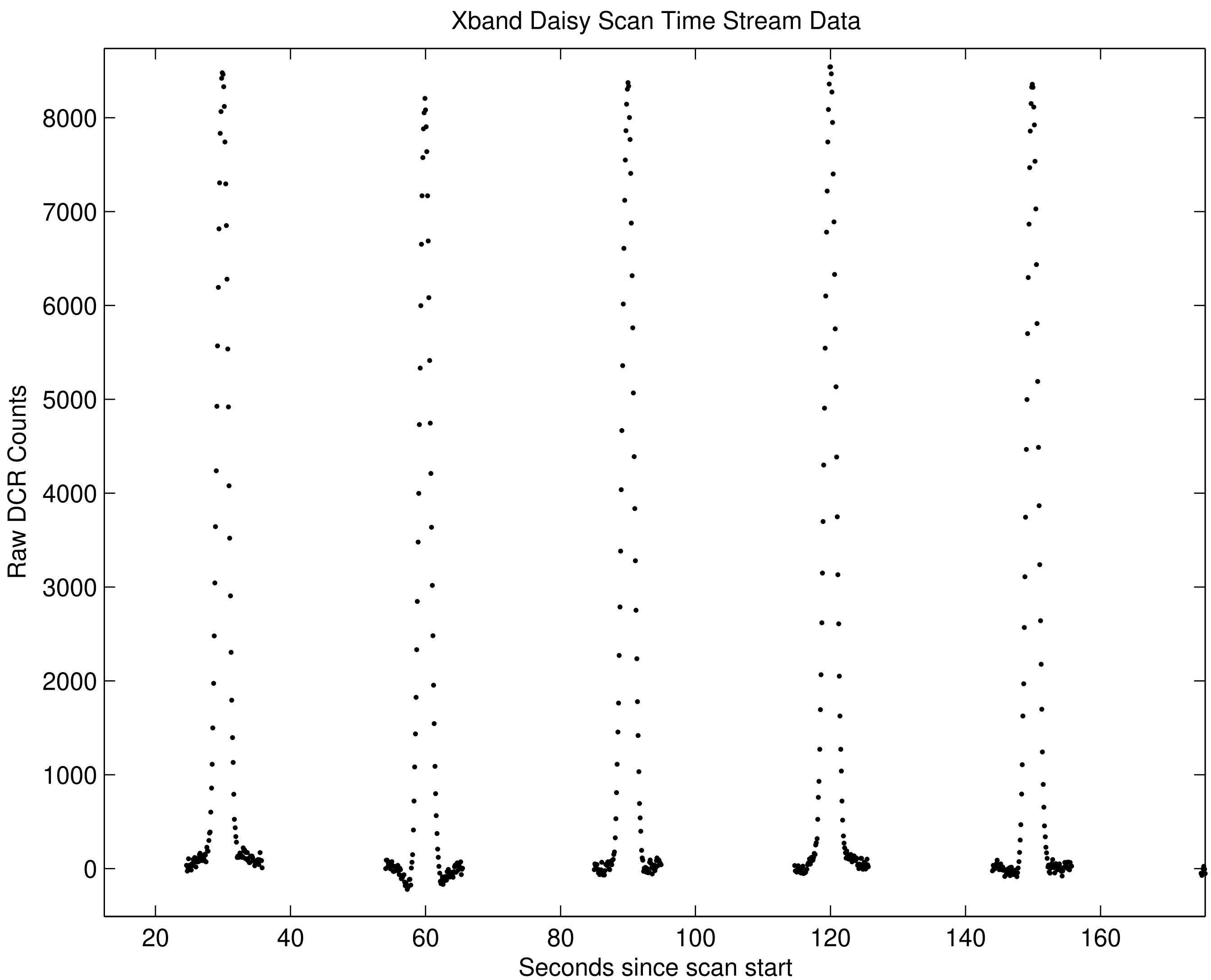

Fig. 11.— A sample of almost-raw DCR data for the daisy scan (number 136). Data outside of a radius of 3 X-band FWHM's is excluded; each remaining ("ON") data chunk has had a mean and gradient independently estimated & removed.

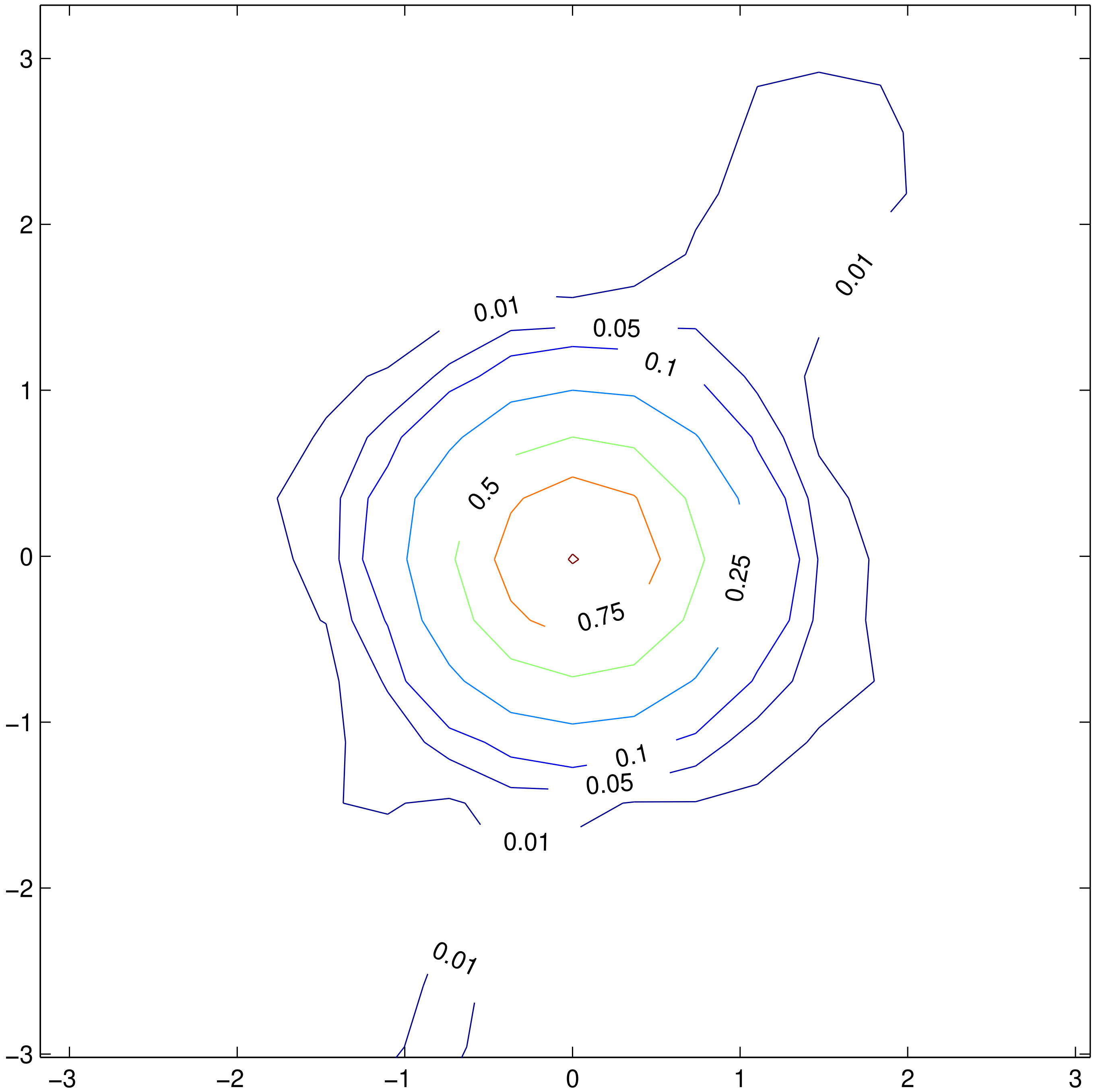

Fig. 12.— X-band beammap made from scan 136. Inspection of the timestream data suggests that atmospheric artifacts persist at the 1% level so the lowest contour is probably not meaningful. Axes are in arcminutes of Commanded Ra/Dec (minus the central Ra/Dec).